Phalloidin Synthetic Analogues: Structural Requirements in the Interaction with F-Actin

Lucia Falcigno,[a, b] Susan Costantini,[a] Gabriella D'Auria,[a, b] Bianca Maria Bruno,[c] Suse Zobeley,[d] Giancarlo Zanotti,[c] and Livio Paolillo*[a, b]

Abstract: Synthetic derivatives of phalloidin have been investigated in solution by circular dichroism (CD) and NMR spectroscopy. They differ from natural phalloidin (PHD), bicyclo(Ala[1]-D-Thr[2]-Cys[3]-*cis*-4-hydroxy-Pro[4]-Ala[5]-2-mercapto-Trp[6]-$(OH)_2$Leu[7])(S-3 → 6), in that they are modified at positions 2, 3, and 7. Among these synthetic analogues, structural differences and varying degrees of atropisomerism are found. By comparing the respective molecular models obtained by restrained molecular dynamics (RMD) simulations based on experimental NMR data, structural features that may be responsible for the different biological behavior become apparent. Our results indicate that the structural changes that result from an inversion of chirality of residue 3 lead to a complete loss of toxicity. Conversely, toxicity is less affected by the structural changes that stem from an inversion of chirality of residue 2. Moreover, unlike the other phallotoxins, when the thioether unit bridges to the opposite face of the main peptide ring, in contrast to the situation in other phallotoxins, large structural changes are observed as well as a total loss of activity. Molecular models of the synthetic phalloidin analogues have been used to investigate the necessary structural requirements for the interaction with F-actin. To this end, the F-actin/PHD model of M. Lorenz et al. was employed; docking experiments of our molecular models in the PHD binding site are presented.

Keywords: atropisomerism · conformation analysis · F-actin · NMR spectroscopy · phallotoxin analogues

Introduction

Amatoxins and phallotoxins are two families of toxic bicyclic peptides isolated from the very dangerous mushroom *Amanita phalloides*.[1]

[a] Prof. L. Paolillo, Dr. L. Falcigno, Dr. S. Costantini, Prof. G. D'Auria
Dipartimento di Chimica
Università di Napoli "Federico II"
Complesso Universitario Monte S. Angelo
via Cinthia, 80126 Napoli (Italy)
Fax: (+39) 081-674090
E-mail: paolillo@chemistry.unina.it

[b] Prof. L. Paolillo, Dr. L. Falcigno, Prof. G. D'Auria
Centro di Studio di Biocristallografia del C.N.R.
Università di Napoli "Federico II", Via Mezzocannone 4
80134 Napoli (Italy)

[c] Dr. B. M. Bruno, Dr. G. Zanotti
Centro di Chimica del Farmaco del CNR
Università di Roma "La Sapienza", Piazzale A. Moro
Roma (Italy)

[d] S. Zobeley
MPI für medizinische Forschung
Ladenburg bei Heidelberg (Germany)

Supporting information for this article is available on the WWW under http://wiley-vch.de/home/chemistry/ or from the author: Tables of carbon chemical shifts (Table S1) from NMR analysis and proton–proton distances (Table S2) from NMR data and RMD calculations.

Amatoxins, the slow acting *Amanita* toxins, are bicyclic octapeptides; the strong 1:1 complexes that they form with RNA Polymerase B blocks protein synthesis, especially in liver and kidneys cells, leading to the fatal necrosis of these organs. The amatoxins are only responsible for the death of patients after ingestion.

Phallotoxins are bicyclic heptapeptides. The main common feature is a transannular thioether bridge between the side chains of their tryptophan and cysteine residues (Figure 1). They are also characterized by the presence of some unusual hydroxylated amino acids.

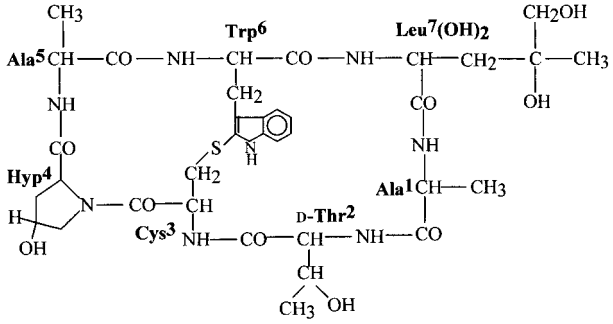

Figure 1. Chemical structure of phalloidin.

The quick-acting phallotoxins lead to death in experimental animals within 2–5 hours after injection, but not after ingestion. Phallotoxins, which are rapidly adsorbed by hepatocytes in vivo as well as in vitro, cause a severe swelling of the liver due to accumulation of blood and hemorrages.[2] The molecular mechanism of action of phallotoxins stems from their strong affinity towards F-actin.[3, 4] They prevent the depolymerization of F-actin into G-actin, so that the physiological equilibrium G-actin $\rightleftharpoons$ F-actin is significantly shifted to the right, depleting cells of G-actin to an intolerable extent. Phallotoxins also stabilize the F-actin filaments against chemical and physical influences.[5–7]

Due to their bicyclic nature, phallotoxins are fairly rigid molecules, characterized by very specific spectroscopic properties that correspond directly to their toxicities. The 2-indolyl thioether moiety, the dissymmetric chromophoric system responsible for the UV spectrum with $\lambda_{max} = 292$ nm and for the characteristic strongly positive Cotton effects in the CD spectrum at around 300 and 240 nm, is positively helical, as demonstrated by the X-ray structure of a related peptide model[8] and recently confirmed by an X-ray analysis of a synthetic bioactive phallotoxin analogue.[9] Any variation from the typical UV and CD spectra exhibited by bioactive phallotoxins is always associated with a notable or even total loss of toxicity.

The three-dimensional structure of phallotoxins has been defined in solution by two-dimensional NMR spectroscopy and molecular dynamics studies,[10–14] and recently in the solid state, by X-ray analysis of a synthetic analogue.[9]

Retaining the necessary bicyclic structure, the influence of the side chain on the affinity towards F-actin has been analyzed by carrying out structure–activity relationship (SAR) studies on both semisynthetic and totally synthetic analogues.[15–18] These studies have shown that the Cys^3, 4-*cis*-hydroxy-Pro^4 (Hyp^4), Ala^5, and Trp^6 residues are essential for toxicity. Only a minor contribution is made by the Ala^1 side chain, which can be varied or even omitted without any significant consequences. The side chain of the residue in the 7-position, a differently hydroxylated leucine in the natural toxins, is the least important for binding to F-actin and can be suitably modified to give biochemically fluorescent analogues useful as sensitive tools for visualizing F-actin in biological tissue.[19, 20] On the other hand, the side chain of the residue in the 2-position, a D-Thr or a β-hydroxy-Asp in the natural products, is essential for actin binding. A D-configuration and a length of at least two carbon atoms for the side chain of this residue are necessary for toxicity;[21, 22] however, the presence of hydroxyl or carboxylic groups has hitherto been considered as unnecessary.

A detailed review of the structure–activity relationships (SAR) of the numerous phallotoxin analogues prepared to date reveals that structural modifications, even those concerning the less sensitive positions, invariably lead to some degree of loss of the affinity towards F-actin.

We report herein on a research project based on the total synthesis of new analogues of the natural phalloidin (PHD), bicyclo(Ala^1-D-Thr^2-Cys^3-*cis*-4-hydroxy-Pro^4-Ala^5-2-mercapto-Trp^6-(OH)$_2$Leu^7)(S-3 $\rightarrow$ 6), a representative phallotoxin (Figure 1), in order to accurately investigate the structural and conformational features known to affect the SAR for this important class of natural biopeptides. Leaving the essential bicyclic structure and the necessary side chains unchanged, we turned our attention to the absolute configuration of the residues in positions 2 and 3, to that of the more versatile side chain of residue 7, and to the not yet fully elucidated role of the side chain of the residue in the 2-position. The new analogues and their affinities towards F-actin are listed in Table 1. Bioactivity was measured as the ability of the analogues to displace [^{3}H]demethylphalloidin from its bound complex with F-actin. Among this series, only those analogues showing a pronounced difference in their affinities towards F-actin with respect to natural phalloidin (specifically **1h**, corresponding to [D-Cys^3,Ala^7]-phalloidin, and **1f** and **1′f**, corresponding to the two atropisomers of [Thr^2,Ala^7]-phalloidin) were selected for conformational analysis in solution.

Table 1. Phalloidin analogues discussed in this paper and their affinity to F-actin.

	Residue 7	Residue 2	Residue 3	Affinity to F-actin (times less than phalloidin)
1a	Ser (Bol)	D-Abu	L-Cys	10
1b	Ala	D-Abu	L-Cys	10
1c	Abu	D-Abu	L-Cys	10
1d	Leu	D-Abu	L-Cys	5.5
1e[a]	Ala	D-Thr	L-Cys	6.2
1f[b]	Ala	L-Thr	L-Cys	>100
1′f[b]	Ala	L-Thr	L-Cys	<100
1g	Leu	D-Thr	L-Cys	1.5
1h	Ala	D-Thr	D-Cys	>100
1i	Ser	D-Abu	L-Cys	10
1j	Ser (caprylyl ester)	D-Abu	L-Cys	10

[a] See ref. [9]. [b] Compounds **1f** and **1′f** are atropisomers.

Results

Synthesis: The new phalloidin analogues were synthesized by using the Savige–Fontana reaction to establish the 2-thioindolyl ether bond through reaction of L-3a-hydroxy-1,2,3,3a,8,8a-hexahydropyrrolo[2,3-*b*]indole-2-carboxylic acid (Hpi)[23] with thiol groups under acidic conditions.[24, 25] This strategy has previously been used to good effect in the total synthesis of analogues of both amatoxins[26, 27] and phallotoxins.[22] The requisite Hpi heptapeptide precursors for cyclization (**3a**–**3h**), bearing acid-labile protecting groups, were synthesized by the classical solution method. As depicted in Scheme 1, on treatment with trifluoroacetic acid (TFA), the protecting groups were cleaved and the thiol reacted intramolecularly with Hpi, to form the monocyclic thioethers (**2a**–**2h**). The subsequent final cyclization reactions afforded the bicyclic analogues (**1a**–**1j**). Only the general procedure for achieving the cyclization reactions is described. Detailed data on the products and their synthesis (Scheme 1) are reported in Tables 2 and 3, respectively.

CD analysis: In general, the thioether bridge constitutes the dissymmetric chromophoric system responsible for the characteristic strongly positive Cotton effects around 300 nm and 240 nm in the CD spectra of phallotoxins.[1]

0947-6539/01/0721-4666 $ 17.50+.50/0 *Chem. Eur. J.* **2001**, *7*, No. 21

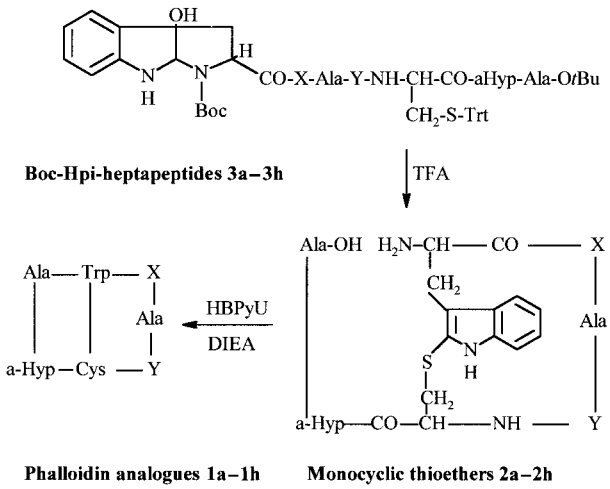

Scheme 1. Synthesis of phalloidin analogues. X and Y correspond to residues 7 and 2, respectively, see Table 1.

Table 2. Conditions for converting Boc-Hpi-heptapeptides (**3a**–**3h**) into monocyclic thioethers (**2a**–**2h**).

	Weight of starting linear heptapeptides [g]	Dissolved in TFA [mL]	Yield [g]	Yield [%]	R_f[a]
2a	0.850	300	0.420	73	0.45
2b	1.300	400	0.500	60	0.50
2c	0.650	250	0.240	60	0.50
2d	0.700	250	0.130	30	0.45
2e	1.200	450	0.410	22	0.45
2f	0.900	500	0.240	40	0.45
2g	0.560	250	0.310	76	0.50
2h	0.800	300	0.250	20	0.45

[a] R_f in *n*-butanol/acetic acid/water (4:1:1).

The CD spectrum of analogue **1h** (Figure 2) shows a positive Cotton effect, specifically, a positive maximum at around 250 nm and two positive maxima at around 292 and 300 nm. This Cotton effect indicates that the value of the indolyl thioether angle is positive (*P* helical).[8] Analogously, the CD spectrum of analogue **1′f** (Figure 2) also shows a positive Cotton effect and *P* helicity.

In contrast, the CD spectrum of analogue **1f** (Figure 2) is the mirror image of that of the natural phalloidin. Thus, it has negative minima at around 250, 292, and 300 nm. This Cotton effect indicates that the indolyl thioether angle is negative (*M* helical).[8]

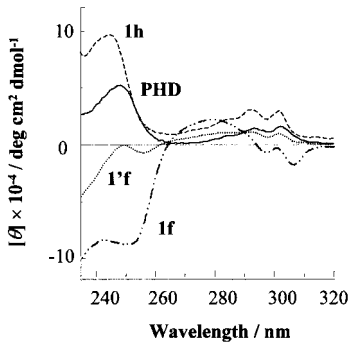

Figure 2. CD spectra of natural phalloidin (PHD) and of the analogues **1h**, **1f**, and **1′f** in CH_3OH.

NMR spectroscopic analysis: For each peptide, proton resonances were assigned with the aid of TOCSY,[28] DQF-COSY,[29, 30] ROESY,[31, 32] and NOESY[33, 34] spectra, while aliphatic and aromatic carbon resonances were assigned by means of HMQC experiments.[35, 36]

All proton spin systems were assigned by following the standard procedure proposed by Wüthrich.[37] Proton chemical shifts of analogues **1h**, **1f**, and **1′f** are reported in Table 4. Prochiral protons were stereospecifically assigned on the basis of the intra-residue NOE effects, such as $H^{\beta} \leftrightarrow NH$ or $H^{\beta} \leftrightarrow H^{\alpha}$, and the $^3J(H^{\alpha},H^{\beta})$ coupling constants obtained from either one-dimensional or DQF-COSY spectra.

The protonated carbons were identified in the HMQC spectrum from the chemical shifts of the directly bound protons. Carbon chemical shifts are available as Supporting Information.

The $^3J(NH,H^{\alpha})$ coupling constants and the experimental Φ values derived from the Karplus-type equation of Bystrov[38] are given in Table 5.

Also included in the same table are the temperature dependences of the amide proton signals, as obtained from one-dimensional spectra recorded between 298 and 310 K. Relatively small temperature coefficients can be noted for the Ala[1] NH (-2.3 ppb K^{-1}) and D-Thr[2] NH (-2.0 ppb K^{-1}) of analogue **1h**, for the Ala[5] NH (-1.1 ppb K^{-1}) of analogue **1f**, and for the Trp[6] NH (-1.5 ppb K^{-1}), Ala[1] NH (-2.3 ppb K^{-1}), and Ala[5] NH (-2.3 ppb K^{-1}) of analogue **1′f**. These data indicate that these protons are likely to be involved in hydrogen bonding.

Structure refinement by molecular dynamics calculations: The conformational analysis of the three phalloidin analogues

Table 3. Conditions for converting monocyclic thioether peptides (**2a**–**2h**) into bicyclic thioether peptides (phalloidin analogues **1a**–**1h**)

	Weight of secopeptides [g]	Dissolved in DMF [mL]	HBPyU [g]	DIEA [g]	Yield [mg]	Yield [%]	R_f[a]	FAB MS $[M-H]^+$
1a	0.420	500	0.220	0.193	38	11	0.50	805
1b	0.570	450	0.215	0.190	20	5.7	0.35	699
1c	0.193	230	0.112	0.100	35	19	0.40	713
1d	0.120	120	0.075	0.060	38	32	0.75	741
1e[b]	0.410	480	0.240	0.280	48	12	0.30	715
1f	0.230	300	0.175	0.150	40[c]	16	0.30	715
1g	0.280	300	0.200	0.180	32	12	0.40	757
1h	0.250	300	0.180	0.155	25	11	0.30	715

[a] R_f in chloroform/methanol/water (65:25:4). [b] See ref. [9]. [c] Composed of two atropisomers (**1f**, **1′f**) in an 80:20 ratio.

Table 4. Proton chemical shifts (δ) of the phalloidin analogues **1h**, **1f**, and **1′f** in [D_6]DMSO at 298 K.

Peptide	Residue	NH	H^{α}	H^{β}	H^{γ}	others
1h	Ala^1	7.61	4.44	1.15		
	D-Thr^2	7.33	4.38	4.01	1.02	
	D-Cys^3	8.43	4.78	2.98 $^{pro-S}$		
				3.45 $^{pro-R}$		
	Hyp^4		4.44	2.00; 2.16	4.10	H^{δ} 3.10; 3.48
	Ala^5	8.08	3.90	0.74		
	Trp^6	7.69	5.34	3.20 $^{pro-S}$		H'_4 7.71; H'_5 6.90; H'_6 7.05;
				3.34 $^{pro-R}$		H'_7 7.20; NH_{ind} 11.11
	Ala^7	8.06	3.98	1.30		
1f	Ala^1	8.67	4.36	1.24		
	Thr^2	6.90	4.26	3.61	1.09	
	Cys^3	9.35	3.28	2.79;3.58		
	Hyp^4		3.22	1.75;2.03	4.11	$O^{\gamma}H$ 4.73; H^{δ} 3.34
	Ala^5	7.94	4.26	1.11		
	Trp^6	5.90	4.17	3.03;3.26		H'_4 7.71; H'_5 6.90; H'_6 7.05;
						H'_7 7.20; NH_{ind} 11.11
	Ala^7	8.15	4.05	1.29		
1′f	Ala^1	7.70	4.39	1.42		
	Thr^2	8.05	3.78	4.25	1.12	
	Cys^3	8.01	4.93	3.38;3.67		
	Hyp^4		4.17	1.86;2.37	4.42	$O^{\gamma}H$ 5.68; H^{δ} 3.68; 3.93
	Ala^5	7.99	3.83	0.74		
	Trp^6	7.34	4.73	3.42		H'_4 7.62; H'_5 7.03; H'_6 7.19;
						H'_7 7.31; NH_{ind} 11.28
	Ala^7	8.18	3.94	1.43		

Table 5. Summary of various parameters for amino acid residues of the phalloidin analogues **1h**, **1f**, and **1′f**: $^3J(NH,H^{\alpha})$ in [D_6]DMSO at 298 K; Φ angles calculated using the Karplus equation; temperature dependence of the NH chemical shifts in $-\Delta\delta/\Delta T$.

Peptide	Residue	$^3J(HN,H^{\alpha})$ [Hz]	$\Phi_{Karplus}$ [°]	$-\Delta\delta/\Delta T$ [ppb K^{-1}]
1h	Ala^1	8.5	−140, −100	2.3
	D-Thr^2	8.0	150, 90	2.0
	D-Cys^3	10.0	120	3.2
	Ala^5	7.0	−160, −80, 60	4.2
	Trp^6	9.7	−120	3.2
	Ala^7	5.0	−165, −60, 20, 100	5.
1f	Ala^1	9.6	−120	2.3
	Thr^2	7.1	−160, −80	−3.2
	Cys^3	2.0	−30, −10, 130, 150	3.2
	Ala^5	9.8	−120	1.1
	Trp^6	7.5	−150, −70	−1.3
	Ala^7	6.7	−160, −80, 50, 70	4.1
1′f	Ala^1	7.6	−150, −90	2.3
	Thr^2	6.8	−160, −80	3.5
	Cys^3	8.8	−140, 100	2.6
	Ala^5	6.2	−160, −70, 40, 80	2.3
	Trp^6	9.0	−130, −110	1.5
	Ala^7	6.2	−160, −70, 40, 80	3.5

is based on the $^3J(H,H)$ coupling constants, the temperature dependence of the NH proton signals, and, in particular, on the ROE effects.

Inter-proton distances computed from cross-relaxation rate values evaluated from the ROESY spectra (σ^R) were used in energy minimization (EM) and restrained molecular dynamics (RMD) simulations, these being more reliable for a correlation time (τ_c) in the nanosecond range.[39] Inter-proton distances are available as Supporting Information.

Bicyclic analogues show different atropisomerism according to whether the thioether bridge is up (U) or down (D) when the peptide chain is followed in a clockwise manner. The thioether bridge in the X-ray structure of analogue **1e**, the only solid-state structure of a phallotoxin so far available and chosen as a starting model for structure calculations, is of the U-type.[9] Consequently, this orientation was initially assumed in the starting model for the three analogues. For analogues **1h** and **1′f**, a very good agreement between the experimental data and the conformational parameters of the molecular model was observed for the U-type structures. In contrast, for analogue **1f**, agreement with the experimental data was only obtained starting from a D-type model.

Molecular model of 1h: The molecular model of peptide **1h**, averaged over the last 50 ps of vacuum RMD calculations, is shown in Figure 3. This model has a U-type structure and a positive value for the indolyl thioether angle (56.3°) according to CD data. Moreover, the model has all peptide bonds other than the Cys^3–Hyp^4 bond in a *trans* configuration.

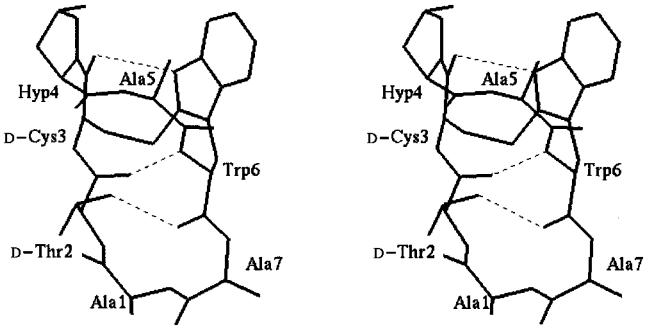

Figure 3. Stereo drawing of the average molecular model of **1h**. The intramolecular H-bonds are indicated as dashed lines.

The backbone dihedral angles (Table 6) are in good agreement with the experimental Φ values reported in Table 5. The occurrence of a type I β-turn in the Trp^6-Ala^7-Ala^1-D-Thr^2 segment would seem to be indicated by dihedral angles in accord with those regularly found in such turns.[40] The experimental NH–NH distances between Ala^1 and D-Thr^2 (2.8 Å) and Ala^1 and Ala^7 (3.1 Å) are also consistent with the presence of a type I β-turn. Moreover, the turn appears to be stabilized by a hydrogen bond between the Trp^6 CO and the D-Thr^2 NH, thereby accounting for the small $\Delta\delta/\Delta T$ value of the D-Thr^2 NH proton signal (Table 5).

As can be seen in Figure 3, the Ala^5 methyl group lies in the anisotropy area of the Trp^6 indole system, a result which is in agreement with the high-field shift of the Ala^5 methyl resonance (Table 4).

Molecular model of 1f: The molecular model of analogue **1f** (Figure 4) shows a D-type structure and a negative value of the indolyl thioether angle (−74.2°), in agreement with CD data. Again, this model has all peptide bonds other than the Cys^3–Hyp^4 bond in a *trans* configuration. A type VIa β-turn in the Thr^2-Cys^3-Hyp^4-Ala^5 segment can be assumed from dihedral angles in accordance with those regularly found in

0947-6539/01/0721-4668 $ 17.50+.50/0 *Chem. Eur. J.* **2001**, *7*, No. 21

Table 6. Backbone angles [°] averaged during the last 50 ps of RMD calculations of **1h**, **1f**, and **1′f** molecular models.

Peptide	Residue	Φ	Ψ	ω
1h	Ala[1]	−115.9	52.9	164.1
	D-Thr[2]	81.9	−159.9	−177.5
	D-Cys[3]	118.7	4.51	164.0
	Hyp[4]	−92.8	6.48	2.99
	Ala[5]	−129.7	18.6	−168.3
	Trp[6]	−119.4	−177.8	−168.0
	Ala[7]	−58.6	−32.1	−174.0
1f	Ala[1]	−175.2	50.1	146.2
	Thr[2]	−165.0	56.7	−179.1
	Cys[3]	−50.1	123.9	178.2
	Hyp[4]	−66.2	−14.0	17.4
	Ala[5]	−92.8	88.0	169.7
	Trp[6]	−78.6	15.5	−154.5
	Ala[7]	−65.2	−33.4	166.8
1′f	Ala[1]	−140.9	−106.1	178.2
	Thr[2]	−71.6	−26.7	−174.1
	Cys[3]	−119.5	124.0	175.3
	Hyp[4]	−53.6	−26.0	−172.7
	Ala[5]	−66.6	−18.0	163.8
	Trp[6]	−120.2	21.1	−171.4
	Ala[7]	63.0	7.16	179.2

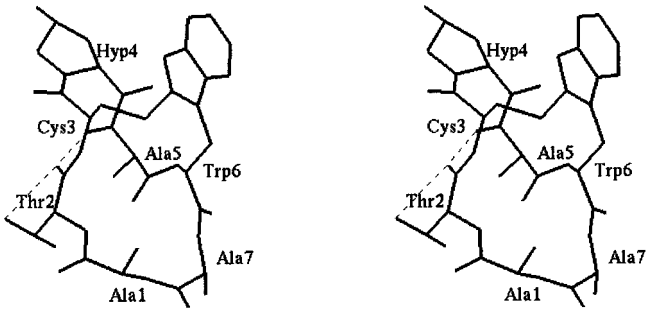

Figure 4. Stereo drawing of the average molecular model of **1f**. The intramolecular H-bonds are indicated as dashed lines.

such turns.[40] The turn is stabilized by a hydrogen bond between the Thr[2] CO and the Ala[5] NH, as indicated by the small $\Delta\delta/\Delta T$ value of the Ala[5] NH proton signal (Table 5).

As can be seen in Figure 4, the Trp indole ring is oriented towards the Hyp[4] and Trp[6] residues, thereby accounting for the high-field shifts of the Hyp[4] H^{α} and Trp[6] NH resonances (Table 4).

Molecular model of 1′f: The molecular model of **1′f**, averaged over the last 50 ps of RMD calculations, is shown in Figure 5.

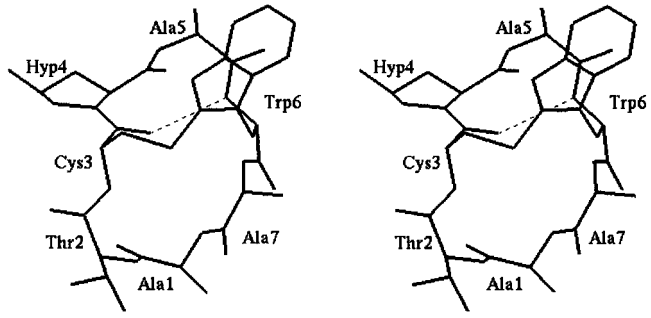

Figure 5. Stereo drawing of the average molecular model of **1′f**. The intramolecular H-bonds are indicated as dashed lines.

This model shows a U-type structure and a positive value for the indolyl thioether angle (131.8°), in agreement with CD data. All peptide bonds are in a *trans* configuration. Considering the backbone dihedral angles (Table 6), which are in good agreement with the experimental Φ values (Table 5), the occurrence of a type I β-turn in the Cys[3]-Hyp[4]-Ala[5]-Trp[6] segment can be inferred.[40] The experimental NH–NH distances between Ala[5] and Trp[6] (2.6 Å) and Ala[5] and Hyp[4] H^{α} (3.3 Å) are also consistent with the presence of a type I β-turn. The turn is stabilized by a hydrogen bond between the Cys[3] CO and the Trp[6] NH, as is also suggested by the small $\Delta\delta/\Delta T$ value of the Trp[6] NH proton signal (Table 5). As can be seen in Figure 5, the Trp indole ring is oriented towards the Hyp[4]-Ala[5] segment, thereby accounting for the high-field shift of the Ala[5] methyl resonance (Table 4).

Discussion

Phalloidin is the main representative member of phallotoxins, a family of toxic bicyclic heptapeptides produced by the poisonous mushroom *Amanita Phalloides*. The mechanism of their toxic effect involves specific binding of the toxin to F-actin in liver cells.

In this study, a comparative conformational analysis of phalloidin synthetic derivatives modified at positions 2, 3, and 7 has been carried out by NMR and RMD methods with a view to elucidating the structural role and the mutual influence of these residues in the interaction with F-actin.

As reported previously, a D-configuration and a side chain composed of at least two carbon atoms for residue 2 are prerequisites for phallotoxin binding to F-actin. The β-hydroxyl or carboxyl groups present on the side chain of residue 2 of natural phallotoxins have hitherto been considered as nonessential for toxicity and have been omitted in synthetic analogues, in which the native D-Thr[2] and D-β-hydroxy-Asp[2] residues have often been replaced by the less expensive and synthetically simpler D-Abu.[19, 20] However, our results indicate that the D-Thr[2] analogues are about two to three times more active than their D-Abu[2] counterparts (**1e** vs **1b** and **1g** vs **1d**; see Table 1). Our findings also establish the role of the hydroxyl group, which is capable of hydrogen-bond formation and thus promotes a further stabilization of the binding to F-actin.

The role of the side chain of residue 7 has been examined, focusing on some hitherto uninvestigated structural properties, such as its length, lipophilic character, the presence of heteroatoms, and branching. To this end, a series of D-Abu[2] analogues was prepared that contain the following residues in the 7-position: L-Ala, L-Abu, L-Leu, and L-Ser (analogues **1b**, **1c**, **1d**, and **1i**, respectively). The benzyl ether and caprylyl ester of **1i** (analogues **1a** and **1j**, respectively) were also prepared and tested. All of these analogues, with the exception of **1d**, were found to exhibit the same reduced affinity to F-actin, amounting to about one-tenth of that of phalloidin itself, thus confirming the high flexibility of this side chain. Only [D-Abu[2],Leu[7]]-phalloidin (**1d**) was found to exhibit a twofold higher affinity towards F-actin. A branched side chain seems the sole requisite of the residue in the

7-position for it to positively influence the toxicity of phallotoxins. Almost complete recovery of the affinity of PHD towards F-actin is realized by combining the positive effects of the D-Thr[2] and Leu[7] residues present in the synthetic [D-Thr[2],Leu[7]]-phalloidin (**1g**). Specifically, 40% and 60% of the recovered bioactivity can be assigned to the β-hydroxyl group on the side chain of D-Thr[2] and to the branched side chain of Leu[7], respectively.

The replacement of D-Thr[2] in the [Ala[7]]-phalloidin (**1e**)[9] by an L-Thr[2] residue (analogues **1f** and **1′f**) causes a pronounced loss of toxicity (Table 1). Analogues **1f** and **1′f** correspond to two atropisomers obtained by two subsequent cyclization reactions of the appropriate linear heptapeptide precursor. They differ from each other in the helipticity of the chromophoric 2-indolyl-thioether moiety.

The most abundant isomer [Thr[2],Ala[7]]-phalloidin (**1f**), for which the CD spectrum is the mirror-image of that of phalloidin, is *M* helical. Its three-dimensional structure, established by means of two-dimensional NMR and computational methods, exhibits significant backbone changes (Figure 4) compared to the bioactive molecular shape of phallopeptides. The molecular model of **1f** is substantially different from all the others since it has a D-type structure. Moreover, **1f** does not show any affinity towards F-actin. Thus, we conclude that the ring closure is likely to be very important in determining the interaction with F-actin.

The less abundant isomer [Thr[2],Ala[7]]-phalloidin (**1′f**) is characterized by a CD spectrum similar to that of phalloidin and, therefore, has the same *P* helipticity. The conformational NMR and RMD analyses confirmed the close analogy of its backbone structure with that of toxic phallopeptides, revealing a U-type structure with a very rigid region (3–6 residues) containing the sulfide bridge, and a more flexible part (2–7 residues).

The synthetic [D-Cys[3],Ala[7]]-phalloidin (**1h**), in which the absolute configuration of residue 3 has been changed, proved to be totally inactive. The CD spectrum of this analogue shows some similarities but also marked differences when compared to those of the bioactive phallopeptides. The three-dimensional structure of this molecule, as determined by two-dimensional NMR and RMD analyses, shows significant structural modifications of the backbone, mainly due to isomerism about the Cys[3]–Hyp[4] peptide bond (*trans* in natural PHD[11] and in the active analogues **1e**[9] and **1′f**; *cis* in **1h**) and the different position of a type I β-turn (residues 3–6 in PHD,[11] **1e**,[9] and **1′f**; residues 6–2 in **1h**). Therefore, the inversion of chirality of residue 3 leads to significant structural changes of the backbone with a concomitant loss of activity.

Structural requirements in the interaction with F-actin: In order to elucidate the interactions of our active analogues with F-actin, we attempted some docking experiments in the phalloidin binding site of the F-actin model proposed by Lorenz et al. in 1993[41] by combining the atomic structure of G-actin[42] and the X-ray fiber diffraction data.[43] The protein data bank (pdb) coordinates of the F-actin model were kindly provided by Michael Lorenz of the Max-Planck Institute, Heidelberg. Attempts at docking were successful with the molecular models of **1e**[9] and **1′f** since these have a close structural resemblance to the molecular model of natural phalloidin.[11]

Average molecular models of **1e** and **1′f** were introduced by superposition on the PHD structure present in the original F-actin model of Lorenz and co-workers, which was rotated by $\approx 180^\circ$ about an axis roughly parallel to the filament axis. Indeed, this was shown to be the preferred orientation for PHD within the F-actin binding site by Steinmetz et al. in 1998[44] on the basis of scanning transmission electron microscopy (STEM) and of a three-dimensional helical reconstruction. In this orientation, phalloidin is capable of binding two or three monomers of the actin helix simultaneously, subject to structural and biochemical constraints.[44]

The three monomers of the actin helix with the molecular model of **1e** (in a red ball-and-stick representation), replacing PHD in its binding site, are shown in Figure 6. F-actin residues likely to be involved in interactions with our compound are

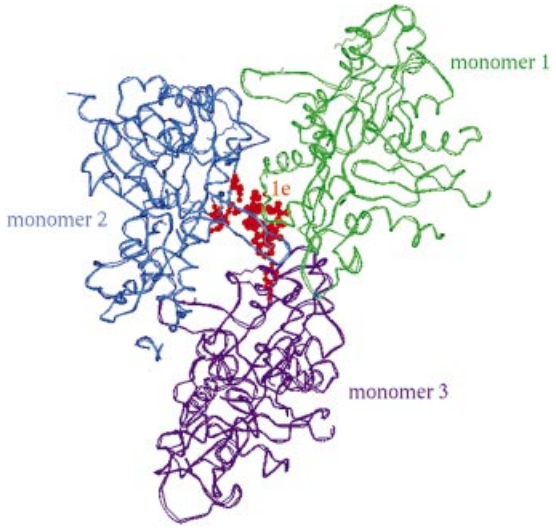

Figure 6. Ribbon representation of PHD/F-actin trimer (data from M. Lorenz et al., 1993)[41] with the molecular model of **1e** (red ball-and-stick) in the PHD binding site. Actin residues likely to interact with the toxin are also displayed in a red ball-and-stick representation.

also displayed in a red ball-and-stick representation. As can be seen from an expansion of the PHD binding site (Figure 7a), Tyr[279] of F-actin monomer 3 (purple) may establish stacking contacts with Trp[6] of **1e**, whilst hydrogen bonds may be formed between Hyp[4] and Thr[77], Glu[72], Asp[179], and Arg[177] of monomer 2 (blue) or between D-Thr[2] and Ser[199] of monomer 1 (green). Significantly, the mutation of Asp[179] and Arg[177] into alanine prevents the binding of PHD to actin,[45] pointing to the crucial role of Hyp[4] in the toxin function.

A further trial was carried out by docking the molecular model of **1′f** within the phalloidin binding site. The molecular models of **1e**[9] and **1′f** show a close similarity (backbone rmsd = 0.64 Å). They both have a U-type structure, with a positive value of the thioether angle and a *trans* Cys[3]–Hyp[4] peptide bond. The main differences stem from the different orientation of the residue 2 side chain owing to the opposite chirality of this residue in the two analogues (D-Thr in **1e**; L-

0947-6539/01/0721-4670 $ 17.50+.50/0 *Chem. Eur. J.* **2001**, *7*, No. 21

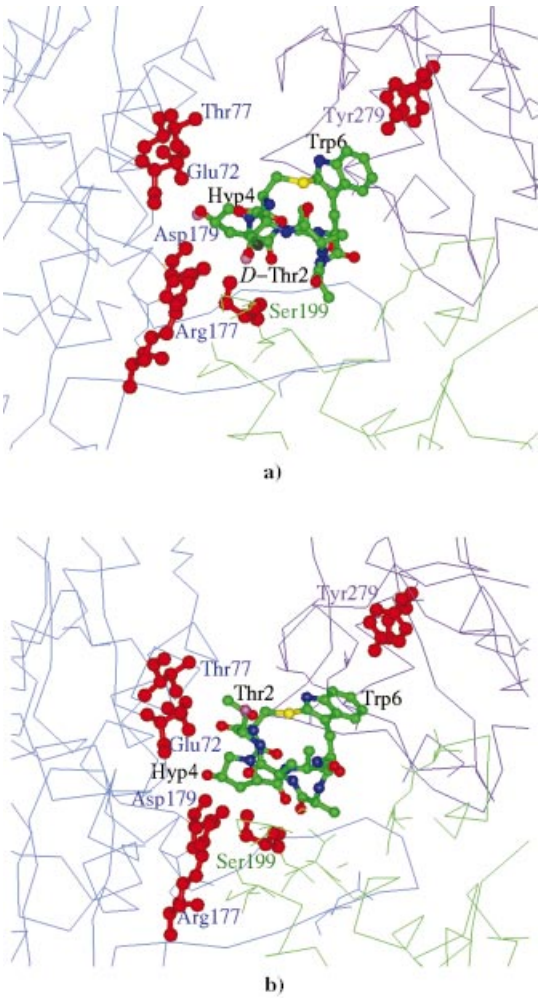

Figure 7. Molecular models of a) **1e** (colored ball-and-stick) and b) **1′f** (colored ball-and-stick) within the PHD/F-actin binding site. PHD was rotated by ≈180°, in contrast to the original Holmes–Lorenz model,[41] as proposed by Steinmetz et al.[44] Actin residues likely to interact with the toxin are labeled and displayed in red ball-and-stick representation.

Thr in **1′f**). On these grounds, it is not surprising that the same interactions between the molecular model of **1′f** and F-actin are discernible, with the sole exception of those involving the L-Thr^2 side chain. In fact, as shown in Figure 7b, the L-Thr^2 O$^\gamma$H (in pink) points away from Ser^{199} of monomer 1 (in green) and, consequently, hydrogen bonds between the toxin and the F-actin monomer 1 are no longer present. Since **1′f** retains some residual affinity towards F-actin, the wrong orientation of the side chain of L-Thr^2 can be regarded as being solely responsible for the large, albeit incomplete, loss of toxicity.

These results cast new light on the interaction mechanism between phallotoxins and F-actin. Although still tentative, this model of interaction may prove to be of considerable help in the rational design of new synthetic peptides of biological and pharmaceutical interest.

Experimental Section

Synthesis: The purities of all the synthesized peptides were checked by thin-layer chromatography (TLC) on precoated silica G-60 plates (Merck 60 F_{254}). Solvent mixtures are indicated in the respective sections. Spots were visualized by means of the ninhydrin reaction, iodine vapor staining, or the color reaction with cinnamaldehyde/HCl gas. The kieselguhr used for preparative separations was from Merck. UV spectra were recorded on a Shimadzu UV-2101 PC spectrophotometer. All peptides gave satisfactory amino acid analyses.

Monocyclic thioether peptides 2a–2h: A solution of the appropriate *tert*-butyloxycarbonyl (Boc) Hpi-heptapeptide **3a–3h** (0.56–1.2 g) in TFA (250–750 mL) was kept at room temperature for 3 h and then concentrated. The residue was thoroughly washed with diethyl ether, dissolved in a little aqueous ammonia (2 M), and purified by chromatography on a 2.5 × 250 cm column of Sephadex LH20 eluting with a solution of NH_4OH (2 mL) in water (1 L). The fractions that eluted after 0.7–1 L eluent had been passed, with a total volume of about 200 mL, were checked by TLC (pale blue with cinnamaldehyde/HCl) and showed the correct UV and CD spectra. The combined fractions were concentrated and the residue was freeze dried. The cyclization conditions, the yields of the cyclization products, and the R_f values of **2a–2h** are given in Table 2.

Bicyclic thioether peptides 1a–1h: A solution of **2a–2h** (0.5 mmol) in dimethylformamide (DMF; 500 mL) was mixed at room temperature with *O*-[benzotriazol-1-yl-*N*,*N*,*N*^{1},*N*^{1}-bis(tetramethylene)uronium hexafluorophosphate] (HBPyU; 0.226 g, 0.525 mmol) and *N*-ethyldiisopropylamine (DIEA; 0.195 g, 1.5 mmol). After stirring overnight at room temperature, the solvent was evaporated in a strong vacuum and the residue was purified by chromatography on a 2.5 × 250 cm column of Sephadex LH20 eluting with methanol. The fractions containing the expected bicyclic peptides were freed of methanol in vacuo, and the residue was further purified by semipreparative high-pressure liquid chromatography (HPLC) with a water/acetonitrile gradient. The cyclization of monocyclic **2f** gave the two atropisomers **1f** and **1′f** in a ratio of 80:20. A dark blue was seen with cinnamaldehyde/HCl. All the bicyclic products, other than **1f** and **1h**, gave a CD spectrum corresponding to that of bioactive phallopeptides, showing positive Cotton effects at around 240 nm and 300 nm. The cyclization conditions, yields of the cyclization products, R_f values, and molecular masses of **1a–1h** are summarized in Table 3.

Bicyclic peptides 1i, 1j: A solution of peptide **1a** (30 mg, 0.036 mmol) in methanol (10 mL) was hydrogenated at room temperature in the presence of 10% Pd/charcoal catalyst (10 mg). After 24 h, the catalyst was filtered off, the filtrate was concentrated, and the residue was purified by chromatography on a 1.5 × 30 cm silica gel column with chloroform/methanol (87:13) as the eluent. Work-up of fractions 25–35 (10 mL) afforded **1i** (20 mg, 75% yield); $R_f = 0.25$ (chloroform/methanol, 9:1); FAB MS: $m/z = 715$ $[M-H]^+$.

Dicyclohexylcarbodiimide (DCCI; 5.1 mg, 0.026 mmol), dimethylaminopyridine (DMAP; 3.6 mg, 0.03 mmol), and caprylic acid (3.6 mg, 0.026 mmol) were added to a solution of **1i** (18.5 mg, 0.026 mmol) in CH_2Cl_2 (3 mL) at 0 °C under stirring. After stirring for 3 days at room temperature, the reaction mixture was concentrated to dryness in vacuo, and the residue was washed repeatedly with diethyl ether and purified by chromatography on a 1.5 × 50 cm silica gel column with chloroform/methanol (87:13) as the eluent. Work-up of fractions 10–12 (10 mL) gave **1j** (5 mg, 23% yield); $R_f = 0.45$ (chloroform/methanol, 9:1); FAB MS: $m/z = 841$ $[M-H]^+$.

CD measurements: CD spectra were recorded with samples in CH_3OH at room temperature by using a Jasco J-715 dichrograph equipped with a Jasco Dp-501 N data processor. Cylindrical fused-quartz cells of pathlength 1 cm were employed. Peptide concentrations were of the order of 10^{-5} M. The molar ellipticities of the peptides in solution ($[\theta]_m$ in deg cm^2 dmol^{-1}) were measured in the wavelength (λ) range 240–320 nm.

NMR measurements: Sample solutions of peptides **1h**, **1f**, and **1′f** were prepared by dissolving each peptide (2.5 mg) in [D_6]DMSO (0.75 mL; Euriso Top, 100% isotopic purity).

^{1}H NMR spectra were recorded on a Varian Unity 400 instrument operating at 400 MHz, located at the "Centro di Studio di Biocristallografia del C.N.R.", University of Naples "Federico II". ^{13}C NMR spectra were acquired on a Bruker DRX instrument operating at a frequency of 100.6 MHz, located at the "Centro Interdipartimentale di Metodologie Chimico-Fisiche", University of Naples "Federico II". The spectra were acquired at 298 K. They were calibrated with respect to [D_6]DMSO (^{1}H: $\delta = 2.50$; ^{13}C: $\delta = 39.5$) as an internal standard. One-dimensional NMR

spectra were recorded with 16 k data points, 32 scans, and a spectral width of 5000 Hz. Two-dimensional NMR experiments, such as DQF-COSY, TOCSY, NOESY, and ROESY were generally recorded with 2048 data points (4096 for DQF-COSY) in *t*2 and 256 data points in *t*1, by the phase-sensitive States–Haberkorn method. FIDs were multiplied by square-shifted sinebell weighting functions in both dimensions and data points were zero-filled to 1024 in *t*1 prior to Fourier transformation. $^3J(NH,H^{\alpha})$ coupling constants were taken from the ^1H NMR spectra and from DQF-COSY spectra in cases of overlapped resonances. The temperature dependences of the amide proton signals were obtained from ^1H spectra recorded in the range 298–310 K.

HMQC spectra were acquired with a GARP decoupling during acquisition, 2048 data points in *t*2 and 256 increments in *t*1 (zero-filled to 512 prior to Fourier transform), a relaxation delay of 3 s, and 128 scans per spectrum.

Two series of NOESY and ROESY spectra were acquired with mixing times of 50, 100, 200, 300, 400 ms and 60, 100, 160, 220 ms, respectively, for each peptide. Off-resonance effects, associated with the low-power spinlock field in the ROESY experiments, were compensated by means of two $\pi/2$ hard pulses before and after the spinlock period.[46] NOE and ROE intensities were evaluated by integration of cross-peak volumes using the appropriate Varian software.

The transformed two-dimensional spectra were baseline-corrected, and then cross- and diagonal-peak volumes were measured. The cross-peak volumes were normalized with respect to the diagonal peaks. A correction was made for the frequency offset effect in the rotating frame.[46] The normalized volumes (A_i) give a linear build-up for short mixing time values up to 0.3 s. The cross-relaxation rates σ_{ij} were calculated from the slopes of the build-up curves. The same procedure was used for both the NOESY and ROESY spectra.

Two separate lists of interproton distances from cross-relaxation rate values evaluated from NOESY (σ^N) and ROESY (σ^R) spectra were generated by considering the following relationship: $r_{ij} = r_{st}(\sigma_{st}/\sigma_{ij})^{1/6}$.[37] As a reference, the Hyp^4-$H^{\beta\beta'}$ peak was chosen, with the reference r_{st} interproton distance of 1.78 Å for analogue **1h** and the cross-peak between the Trp^6 indole NH proton and the H'_7 proton for analogues **1f** and **1′f**, with the reference r_{st} interproton distance of 2.82 Å.

Structure calculations: Molecular dynamics simulations were performed on a Silicon Graphics INDIGO2 workstation. The INSIGHT/DISCOVER (Biosym Technologies, San Diego, CA, U.S.A.) program with the Consistent Valence Force Field (CVFF)[47] was employed for energy minimizations (EM) and molecular dynamics (MD). The X-ray structure of analogue **1e**[9] was taken as the starting model and residues were appropriately changed on the basis of different amino acid sequences. For each peptide, the initial structure was relaxed over 500 steps of restrained conjugate gradient EM,[48, 49] imposing ROE data as restraints on interproton distances. Interproton distances evaluated from ROE effects were introduced as restraints with a 10% tolerance during the simulations.[50] Pseudoatoms were used instead of those protons that could not be stereospecifically assigned.[51]

The restrained molecular dynamics (RMD) simulations were performed in vacuo at 300 K with 0.5 fs time steps. The motion equation algorithm was of the leapfrog type.[52] The RMD simulations were carried out for 50 ps in the equilibration phase and for 160 ps without velocity rescaling; the temperature was kept constant at 300 K. Data recorded during the last 50 ps of the simulation were used for the statistical analyses.

Acknowledgements

The authors are grateful to Dr. Graeme Nicholson (University of Tübingen, Germany) for performing the racemization tests of the phalloidin synthetic analogues.

[1] T. Wieland, *Peptides of Poisonous Amanita Mushrooms*, Springer, New York, **1986**.
[2] M. Frimmer, *Biol. Unserer Zeit* **1979**, *9*, 147–152.
[3] T. Wieland, *Naturwissenschaften* **1977**, *64*, 303–309.
[4] J. Vandekerckhove, A. Deboden, M. Nassal, T. Wieland, *EMBO J.* **1985**, *4*, 2815–2828.
[5] P. Dancker, J. Low, W. Hasselbach, T. Wieland, *Biochim. Biophys. Acta* **1975**, *400*, 407–414.
[6] J. Low, P. Dancker, T. Wieland, *FEBS Lett.* **1975**, *54*, 263–265.
[7] J. De Vries, T. Wieland, *Biochemistry* **1978**, *17*, 1965–1968.
[8] T. Wieland, B. Beijer, A. Seeliger, J. Dabrowski, G. Zanotti, A. E. Tonelli, A. Gieren, B. Dederer, V. Lamm, E. Haedicke, *Liebigs Ann. Chem.* **1981**, 2318–2334.
[9] G. Zanotti, L. Falcigno, M. Saviano, G. D'Auria, B. M. Bruno, T. Campanile, L. Paolillo, *Chem. Eur. J.* **2001**, *7*, 1479–1485.
[10] N. Kobayashi, S. Endo, H. Kobayashi, H. Faulstich, T. Wieland, *Eur. J. Biochem.* **1995**, *232*, 726–736.
[11] H. Kessler, T. Wein, *Liebigs Ann. Chem*. **1991**, 179–184.
[12] P. Boenzli, J. T. Gerig, *J. Am. Chem. Soc.* **1990**, *112*, 3719-3726.
[13] E. Munekata, N. Kobayashi, S. Endo, H. Faulstich, T. Wieland, in *Peptide Chemistry 1990* (Ed.: Y. Shimonishi), Osaka, **1991**, pp. 333–338.
[14] D. J. Patel, A. E. Tonelli, P. Pfaender, H. Faulstich, T. Wieland, *J. Mol. Biol.* **1973**, *79*, 185–196.
[15] F. Fahrenholz, H. Faulstich, T. Wieland, *Liebigs Ann. Chem.* **1971**, *743*, 89–104.
[16] E. Munekata, H. Faulstich, T. Wieland, *J. Am. Chem. Soc*. **1977**, *99*, 6151–6153.
[17] E. Munekata, H. Faulstich, T. Wieland, *Liebigs Ann. Chem.* **1978**, 776–784.
[18] E. Munekata, H. Faulstich, T. Wieland, *Liebigs Ann. Chem.* **1979**, 1020–1027.
[19] T. Wieland, A. Deboden, H. Faulstich, *Liebigs Ann. Chem.* **1980**, 416–424.
[20] L. S. Barak, R. R. Yocum, *Anal. Biochem.* **1981**, *110*, 31–38.
[21] H. Heber, H. Faulstich, T. Wieland, *Int. J. Pept. Protein Res.* **1974**, *6*, 381–384.
[22] T. Wieland, T. Miura, A. Seeliger, *Int. J. Pept. Protein Res.* **1983**, *21*, 3–10.
[23] W. E. Savige, *Aust. J. Chem.* **1975**, *28*, 2275–2287.
[24] W. E. Savige, A. Fontana, *J. Chem. Soc. Chem. Commun.* **1976**, 600–601.
[25] W. E. Savige, A. Fontana, *Int. J. Pept. Protein Res.* **1980**, *15*, 102–112.
[26] G. Zanotti, C. Birr, T. Wieland, *Int. J. Pept. Protein Res.* **1981**, *18*, 162–168.
[27] G. Zanotti, C. Moebringer, T. Wieland, *Int. J. Pept. Protein Res.* **1987**, *30*, 450–459.
[28] L. Braunschweiler, R. R. Ernst, *J. Magn. Reson.* **1983**, *53*, 521–528.
[30] U. Piantini, O. W. Sørensen, R. R. Ernst, *J. Am. Chem. Soc*. **1982**, *104*, 6800–6801.
[29] M. Rance, O. W. Sørensen, G. Bodenhausen, G. Wagner, R. R. Ernst, K. Wüthrich, *Biochem. Biophys. Res. Commun.* **1983**, *117*, 479–485.
[31] A. Bothner-By, R. L. Stephens, J.-M. Lee, C. D. Warren, R. Jeanloz, *J. Am. Chem. Soc.* **1984**, *106*, 811–813.
[32] A. Bax, D. Davis, *J. Magn. Reson.* **1985**, *63*, 207–213.
[33] A. Kumar, G. Wagner, R. R. Ernst, K. Wüthrich, *J. Am. Chem. Soc.* **1981**, *103*, 3654–3658.
[34] D. Neuhaus, M. Williamson, *The Nuclear Overhauser Effect in Structural Conformation Analysis*, VCH, New York, **1989**.
[35] L. Mueller, *J. Am. Chem. Soc.* **1979**, *101*, 4481–4484.
[36] A. Bax, R. H. Griffey, B. L. Hawkins, *J. Magn. Reson.* **1983**, *55*, 301–315.
[37] K. Wüthrich, *NMR of Proteins and Nucleic Acids*, Wiley, New York, **1986**.
[38] V. F. Bystrov, *Prog. Nucl. Magn. Reson. Spectrosc.* **1976**, *10*, 41–82.
[39] C. Isernia, L. Paolillo, E. Russo, A. L. Pastore, G. Zanotti, S. Macura, *J. Biomol. NMR* **1992**, *2*, 573–582.
[40] G. D. Rose, L. M. Gierasch, J. A. Smith, in *Advances in Protein Chemistry*, *Vol. 37* (Eds.: C. B. Anfisen, J. T. Edsael, F. M. Richards), Academic Press, Orlando, Florida, **1985**, pp. 1–109.
[41] M. Lorenz, D. Popp, K. C. Holmes, *J. Mol. Biol.* **1993**, *234*, 826–836.
[42] W. Kabsch, H. G. Mannherz, D. Suck, E. Pai, K. C. Holmes, *Nature* **1990**, *347*, 37–44.
[43] K. C. Holmes, D. Popp, W. Gebhard, W. Kabsch, *Nature* **1990**, *347*, 44–49.
[44] M. O. Steinmetz, D. Stoffler, S. A. Müller, W. Jahn, B. Wolpensinger, K. N. Goldie, A. Engel, H. Faulstich, U. Aebi, *J. Mol. Biol.* **1998**, *276*, 1–6.

  0947-6539/01/0721-4672 $ 17.50+.50/0

[45] D. G. Drubin, H. D. Jones, K. F. Wertmann, *Mol. Biol. Cell.* **1993**, *4*, 1277–1294.
[46] C. Griesinger, R. R. Ernst, *J. Magn. Reson.* **1987**, *75*, 261–271.
[47] S. Lifson, A. T. Hagler, P. Damber, *J. Am. Chem. Soc.* **1979**, *101*, 5111–5131.
[48] R. Fletcher, C. M. Reeves, *Comput. J.* **1964**, *7*, 149–154.
[49] W. F. van Gunsteren, M. Karplus, *J. Comput. Chem.* **1980**, *1*, 266–274.
[50] W. F. van Gunsteren, H. J. C. Berendsen, *Angew. Chem.* **1990**, *101*, 1020–1051; *Angew. Chem. Int. Ed. Engl.* **1990**, *29*, 992–1023.
[51] K. Wüthrich, M. Billeter, W. Brown, *J. Mol. Biol.* **1983**, *169*, 949–961.
[52] C. L. Brooks III, B. Montgomery Pettitt, M. Karplus, *Advances in Chemical Physics*, *Vol. LXXI*, Wiley, New York, **1988**, Chapter 4, pp. 33–37.

Received: March 30, 2001 [F3166]